

# NJC

Accepted Manuscript



This is an *Accepted Manuscript*, which has been through the Royal Society of Chemistry peer review process and has been accepted for publication.

*Accepted Manuscripts* are published online shortly after acceptance, before technical editing, formatting and proof reading. Using this free service, authors can make their results available to the community, in citable form, before we publish the edited article. We will replace this *Accepted Manuscript* with the edited and formatted *Advance Article* as soon as it is available.

You can find more information about *Accepted Manuscripts* in the [Information for Authors](#).

Please note that technical editing may introduce minor changes to the text and/or graphics, which may alter content. The journal's standard [Terms & Conditions](#) and the [Ethical guidelines](#) still apply. In no event shall the Royal Society of Chemistry be held responsible for any errors or omissions in this *Accepted Manuscript* or any consequences arising from the use of any information it contains.

1 **Highly sensitive fluorescent determination of sulfide using**  
2 **BSA-capped CdS quantum dots**

3 Weidan Na, Xiaotong Liu, Tianyu Hu and Xingguang Su \*

4

5

6

7

8

9

10

11

12

13

14

15

16

17

18

19

20

21

22

23

24

25

26

27 *Department of Analytical Chemistry, College of Chemistry, Jilin University, Changchun, 130012,*

28 *China*

29 \*Corresponding author, Tel.: +86-431-85168352, E-mail address: [suxg@jlu.edu.cn](mailto:suxg@jlu.edu.cn)

30 This work presented a novel nanosensor for rapidly detection of sulfide, which was based on the  
31 fluorescence “turn off-on” of bovine serum albumin-capped CdS quantum dots (BSA-CdS QDs).  
32  $\text{Cd}^{2+}$  could react with  $\text{S}^{2-}$  to generate fluorescent CdS QDs in the presence of BSA. When  $\text{Pb(II)}$   
33 was added to the BSA-CdS QDs solution, the fluorescence of CdS QDs would “turn off” due to  
34 the coordination of the  $\text{Pb(II)}$  and BSA presented on the CdS QDs surface. The quenched  
35 fluorescence of CdS QDs could be “turn on” upon the addition of sulfide by forming the stable  
36  $\text{PbS}$  compound. Quantitative analysis was performed by monitoring the fluorescence intensity  
37 variation of CdS QDs. Under the optimum conditions, a good linear range for sulfide detection  
38 from 0.16-4.8  $\mu\text{mol/L}$  was realized. With the detection limit down to  $5.0 \times 10^{-8}$  mol/L, the  
39 nanosensor exhibited good selectivity for sulfide in the presence of other anions.

40

41 **Key words** sulfide anions; fluorescence detection; CdS quantum dots

42

## 43 1. Introduction

44 Sulfide is widely present in many environments, as sulfide anions are generated not only as a  
45 byproduct from industrial processes but also in bio systems.<sup>1</sup> Sulfide is widely used in different  
46 fields, for instance, conversion into sulfur and sulfuric acid, dyes and cosmetic manufacturing,  
47 production of wood pulp.<sup>2</sup> Exposure to a high level of sulfide can cause adverse effects on human  
48 health including loss of consciousness, irritation of mucous membranes, and respiratory paralysis.  
49 Once protonated, sulfide anions turns into  $\text{HS}^-$  or  $\text{H}_2\text{S}$  which are more toxic and caustic. Recent  
50 studies have shown that protonated sulfide is involved in multiple physiological processes. For  
51 example, cause a reduction in blood pressure, inhibition of insulin signaling and regulation of  
52 inflammation.<sup>3-5</sup> In addition, it is related to several diseases, such as Alzheimer's disease, Down's  
53 syndrome, diabetes, and liver cirrhosis.<sup>6,7</sup> Because of the widely spread of sulfide anions and the  
54 hazardous effect to both humans and other organisms, the development of selective and sensitive  
55 detection of sulfide has attracted increasing attentions.

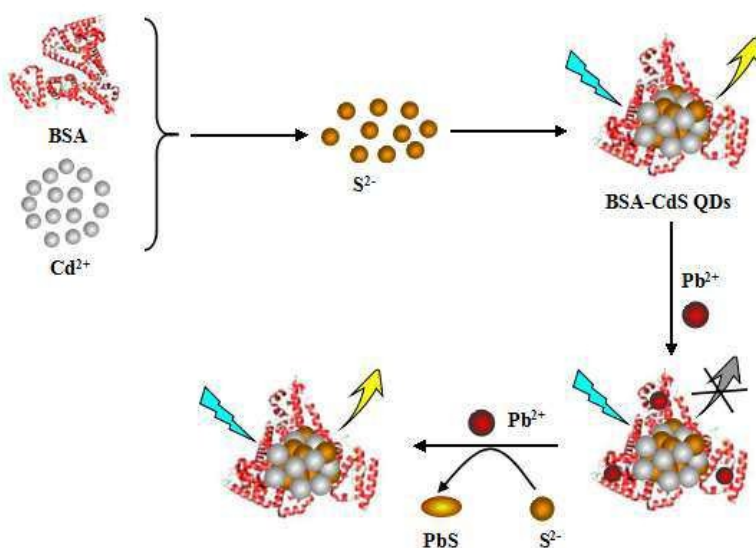
56 Up to date, many strategies have been proposed for the detection of sulfide anions, Whereas  
57 the most useful and effective method for sulfide anions detection are the fluorescence-based  
58 methods. Recently, several groups have made great progress in the development of fluorescence

59 probes for monitoring sulfide anions. These probes are mainly based on specific sulfide induced  
60 reactions, including quencher (such as copper(II)) removal,<sup>8-10</sup> azide reduction,<sup>11-13</sup> nitro reduction  
61 <sup>14</sup> and nucleophilic reaction <sup>15,16</sup> to achieve a fluorescent turn-on response. Zhang et al. designed  
62 and synthesized a highly luminescent Ru(II)-bipyridine complex. It could react with Cu<sup>2+</sup> to form  
63 a hetero bimetallic Ru(II)-Cu(II) complex, the luminescence was strongly quenched through an  
64 excited-state electron transfer mechanism. In the presence of sulfide, due to the high affinity of S<sup>2-</sup>  
65 to Cu<sup>2+</sup>, stable CuS was formed and the luminescence of the Ru(II) complex was restored [8]. Ye  
66 et al. designed and synthesized a dinuclear ruthenium(II)-copper(II) complex,  
67 [Ru(bpy)<sub>2</sub>(phen-cyc)Cu](PF<sub>6</sub>)<sub>4</sub>, with weakly luminescence, which could rapidly react with H<sub>2</sub>S  
68 and give a strong red luminescence signal in aqueous media.<sup>9</sup> These luminescent probes could be  
69 used for the rapid and accurate detection of sulfide anions. However, the development of such  
70 chemical compounds usually requires a whole set of sophisticated organic reactions and  
71 purification. Probes bearing these functional group usually have the low solubility in aqueous  
72 solution which needs organic solvents for sulfide anions detection.

73 Semiconductor quantum dots (QDs) have generated marvelous interest in the fields of  
74 physics, chemistry and biology owing to their ideal optical properties in the past decade. As a class  
75 of fluorescence probe, QDs with variable surface capping ligands have been extensively used for  
76 cell labeling, tumor imaging and clinical diagnosis in biology and medicine.<sup>17,18</sup> They are usually  
77 used to detect cations such as Pb<sup>2+</sup>, Cd<sup>2+</sup> and Hg<sup>2+</sup> via analyte-induced changes in  
78 photoluminescence in aqueous solution.<sup>19</sup> Recently, QDs have been applied to the detection of  
79 anions as well. Gore et al. designed a simple fluorescent probe for the direct detection of sulfide  
80 anions by virtue of the fluorescence quenching of MPA-capped CdS QDs.<sup>20</sup> Rajabi et al. reported  
81 a simple, fast precipitation method for preparing the ultra-small Zn<sub>0.96</sub>Mn<sub>0.04</sub>S quantum dots in  
82 aqueous media, whose fluorescence could be effectively quenched by sulfide anions via the  
83 effective electron transfer from QDs to sulfide anions.<sup>21</sup> The QDs-based methodology are simple  
84 and quite straightforward and could realized a comparative low detection limit.

85 In this work, we presented a novel sensing method by using CdS QDs-based receptor for  
86 sulfide anions recognition. As shown in Scheme 1, the fluorescent CdS QDs could be generated in  
87 the presence of Cd<sup>2+</sup>, S<sup>2-</sup> and BSA. The BSA served as the capping molecule and was employed to  
88 render the CdS QDs stable against aggregation and water-soluble. As well-known, the

89 fluorescence properties of QDs had a close connection to the composition of surface capped layers.  
90 Abundant amino groups, 34 disulfide bond and 1 thiol existed on the BSA of QDs, thus, the  
91 surface of the BSA-CdS QDs could effectively bind  $Pb^{2+}$  via forming  $Pb^{2+}$ /BSA-CdS complex,  
92 which could lead to the fluorescence quenching via a charge transfer process on the surface of the  
93 QDs. The addition of  $S^{2-}$  anions could turn on the fluorescence of BSA-CdS QDs, because  $S^{2-}$   
94 could snatch the  $Pb^{2+}$  ions from the  $Pb^{2+}$ /BSA-CdS complex to form more stable PbS. Due to the  
95 relatively easy design and convenient handling, we developed a novel fluorescence probe for rapid  
96 and highly sensitive detection of sulfide.



97  
98  
99

100 **Scheme 1** Schematic illustration of the BSA-CdS QDs-based sensing system for sulfide detection.

101

## 102 2. Experimental section

### 103 2.1 reagents

104 All reagents were of at least analytical grade. The water used in all experiments had a resistivity  
105 higher than 18 MΩ cm<sup>-1</sup>. Cadmium (II) chloride (CdCl<sub>2</sub>), sodium hydroxide (NaOH),  
106 Sodiumsulfide nonahydrate (Na<sub>2</sub>S•9H<sub>2</sub>O), trihydroxymethyl aminomethane (Tris) and  
107 hydrochloric acid were purchased from Beijing Chemical Works. Lead (II) and Bovine serum  
108 albumin were purchased from Sigma-Aldrich Corporation. The 0.1 mol/L Tris-HCl buffered

109 solution (pH 8.2) was used as the medium for detection process.

## 110 **2.2 Apparatus**

111 The fluorescence spectra were obtained by using a Shimadzu RF-5301 PC  
112 spectrofluorophotometer equipped with a xenon lamp using right-angle geometry. UV-vis  
113 absorption spectra were obtained by a Varian GBC Cintra 10e UV-vis spectrometer. In both  
114 experiments, a 1 cm path-length quartz cuvette was used. FT-IR spectra were recorded with a  
115 Bruker IFS66V FT-IR spectrometer equipped with a DGTS detector. All pH measurements were  
116 made with a PHS-3C pH meter. Transmission electron microscopy (TEM) experiments were  
117 performed on a Philips Tecnai F20 TEM operating at 200 KV acceleration voltage. The X-Ray  
118 powder Diffraction (XRD) patterns were obtained by a Empyrean XRD. Samples used for XRD  
119 measurements were solid powders prepared by drying the QD precipitate in vacuum.

120

## 121 **2.3 Preparation of BSA-CdS QDs**

122 BSA-CdS QDs were synthesized in aqueous solution. 300  $\mu\text{L}$  2.4 mmol/L BSA solution, 120  $\mu\text{L}$   
123 50 mmol/L  $\text{CdCl}_2$  solution and 0.1 mol/L Tris-HCl buffer (pH 8.2, 150  $\mu\text{L}$ ) were added into 2 mL  
124 calibrated test tube, and shaken thoroughly for 10 minutes. After that, 90  $\mu\text{L}$  30 mmol/L  $\text{Na}_2\text{S}$   
125 solution was added into the test tube and diluted to 1500  $\mu\text{L}$  with deionized water followed by the  
126 thoroughly shaking and equilibrated for 15 minutes. All the reaction conditions for the preparation  
127 of BSA-CdS QDs have been optimized. 50  $\mu\text{L}$  BSA-CdS QDs was diluted to 1500  $\mu\text{L}$  with  
128 deionized water. The fluorescence spectra were recorded from 405 nm to 650 nm with the  
129 excitation wavelength of 340 nm. The slit widths of excitation and emission were both 10 nm.

## 130 **2.4 The quenching effect of $\text{Pb}^{2+}$ on the BSA-CdS QDs**

131 The BSA-CdS QDs solution (50  $\mu\text{L}$ ), 0.1mol/L Tris-HCl buffer (pH 8.2, 150 $\mu\text{L}$ ), and different  
132 amount of  $\text{Pb}^{2+}$  was added into a 2.0 mL calibrated test tube. Then, the solution was diluted to  
133 1500  $\mu\text{L}$  with deionized water followed by the thoroughly shaking and equilibrated for 2 min until  
134 the solution was fully mixed. The fluorescence spectra were recorded from 405 nm to 650 nm  
135 with the excitation wavelength of 340 nm. The slit widths of excitation and emission were both 10

136 nm.

### 137 **2.5 The detection of sulfide**

138 15  $\mu\text{mol/L}$   $\text{Pb}^{2+}$  was added to a 2ml test tube containing 50  $\mu\text{L}$  BSA-CdS QDs solution and 10  
139 mmol pH 8.2 Tris-HCl buffer, and the mixture was incubated for 2 min. Different concentrations  
140 of sulfide were successively added into the calibrated test tube and diluted to the 1.5mL mark with  
141 deionized water followed by the thoroughly shaking. The other process was the same as that in the  
142 detection of  $\text{Pb}^{2+}$ . The fluorescence (FL) intensity of the maximum emission peak was used for the  
143 quantitative analysis of sulfide.

### 144 **2.6 Disposal of lake water sample**

145 The lake water samples were obtained from the Nanhu lake in Changchun. The lake water samples  
146 were filtered several times through qualitative filter paper before analysis and different  
147 concentrations of sulfide were added to prepare the spiked samples.

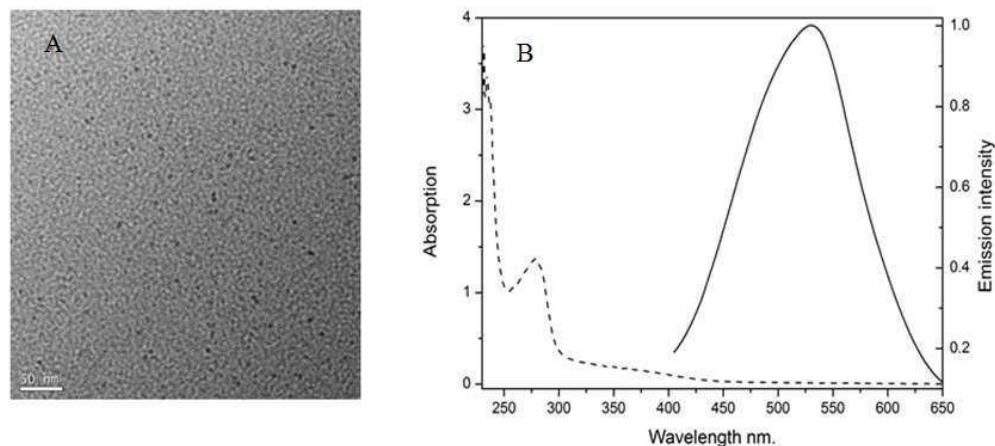
## 148 **3. Results and Discussion**

### 149 **3.1 Spectra of the BSA-CdS QDs**

150 TEM image in Fig. 1(A) revealed the shape of BSA-CdS QDs was nearly spherical with the  
151 average diameter of 6 nm. As shown in Fig. 1(B), there was an increased absorption below 300 nm  
152 and a shoulder around 279 nm that was the result of  $1\text{S}_h-1\text{S}_e$  excitonic transition characteristic of  
153 CdS QDs.<sup>22</sup> The fluorescence emission spectra of the BSA-CdS QDs showed a fluorescent peak  
154 with maximum emission wavelength of 529 nm which arised from excitonic emission of CdS  
155 QDs.<sup>23, 24</sup> The results of XRD studies of the BSA-CdS QDs shown in Fig. S1, the (111), (220), and  
156 (311) planes are clearly distinguishable in the pattern. It is evident from the figure that the crystal  
157 structure of the BSA-CdS QDs is cubic.<sup>25</sup>

158

159



160

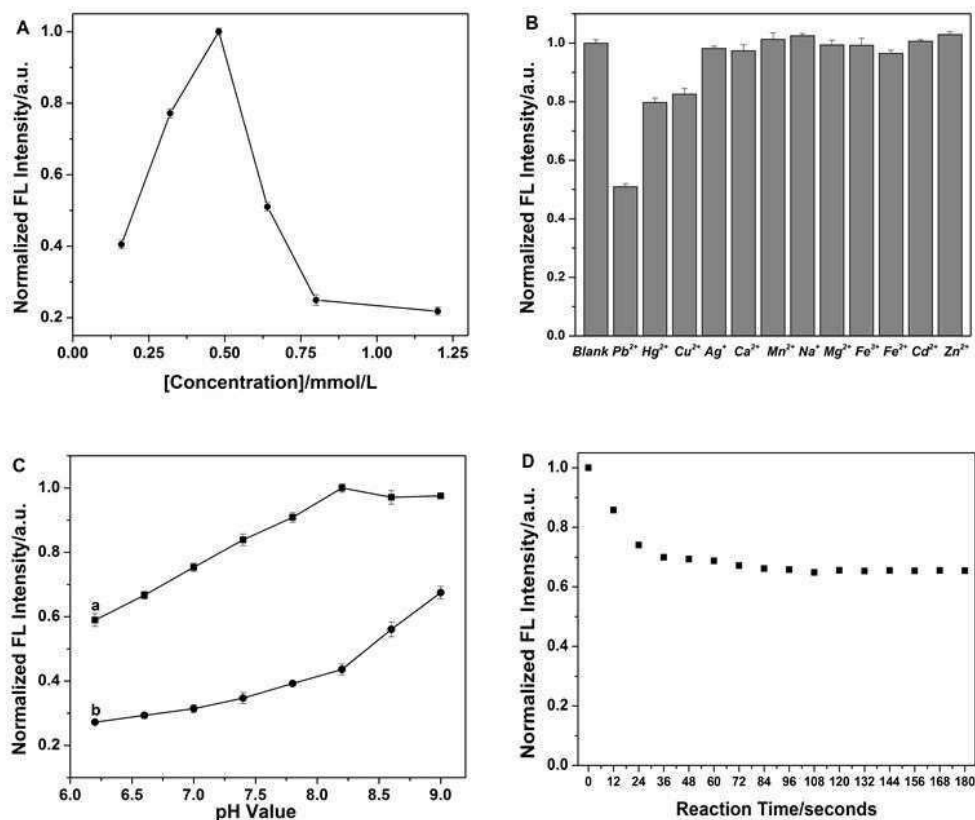
161 **Fig. 1(A)** TEM image of BSA-CdS QDs. **(B)** The UV-vis absorption (Dash line) and fluorescence  
162 emission spectra (Solid line) of BSA-CdS QDs.

163

164 The FT-IR spectra of the CdS crystals with and without BSA as stabilizers were compared to  
165 confirm the coordination of the BSA on the surface of the CdS QDs. As shown in the Figure S2  
166 curve b, the majority of BSA functional groups could be clearly found through the amide I band  
167 ( $1657\text{ cm}^{-1}$ ), amide II ( $1540\text{ cm}^{-1}$ ) band and amide III ( $1400\text{--}1200\text{ cm}^{-1}$ ) for  $-\text{CONH}$  group, which  
168 were the characteristic peak of BSA.<sup>26,27</sup> The disappearance of peaks around  $2590\text{--}2550\text{ cm}^{-1}$ ,  
169 which is actually corresponding to the S-H bond, supports the formation of Cd-S bonds on the  
170 QDs surface. In addition, peaks observed at  $656\text{ cm}^{-1}$  indicates the presence of Cd-S bonds.<sup>24</sup> And  
171 these characteristic peaks were not observed in the FT-IR spectra of uncapped CdS crystals  
172 (Figure S2 curve a) which indicated the successful capping of BSA on the surface of the CdS QDs.

173 **3.2 The optimization**





174

175 **Fig. 2(A)** The FL intensity of BSA-CdS QDs with different BSA concentrations (0.24, 0.36, 0.48,  
 176 0.64, 0.80, 1.20 mmol/L ). **(B)** The quenching effect of 10  $\mu\text{mol/L}$  Pb<sup>2+</sup> or 50  $\mu\text{mol/L}$  Hg<sup>2+</sup>, Cu<sup>2+</sup>,  
 177 Ag<sup>+</sup>, Ca<sup>2+</sup>, Mn<sup>2+</sup>, Na<sup>+</sup>, Mg<sup>2+</sup>, Fe<sup>3+</sup>, Fe<sup>2+</sup>, Cd<sup>2+</sup> and Zn<sup>2+</sup> on the fluorescence of BSA-CdS QDs. **(C)**  
 178 Fluorescence intensity of BSA-CdS QDs assay system without Pb<sup>2+</sup> (curve a) and with 10  $\mu\text{mol/L}$   
 179 Pb<sup>2+</sup> (curve b) in different pH environments (pH 6.2-9.0). **(D)** The quenching effect of Pb<sup>2+</sup> on the  
 180 fluorescence of BSA-CdS QDs at different incubation time.

181

182 Firstly, we studied the effect of the concentrations of BSA on the FL intensity of BSA-CdS QDs.  
 183 As shown in Fig. 2(A), the FL intensity of BSA-CdS QDs increased dramatically with the increase  
 184 of the concentration of BSA in the range from 0.24 to 0.48 mmol/L and decreased rapidly when  
 185 the concentrations of BSA was higher than 0.48 mmol/L. The results indicated that the optimal  
 186 concentration of BSA used for BSA-CdS QDs was 0.48 mmol/L.

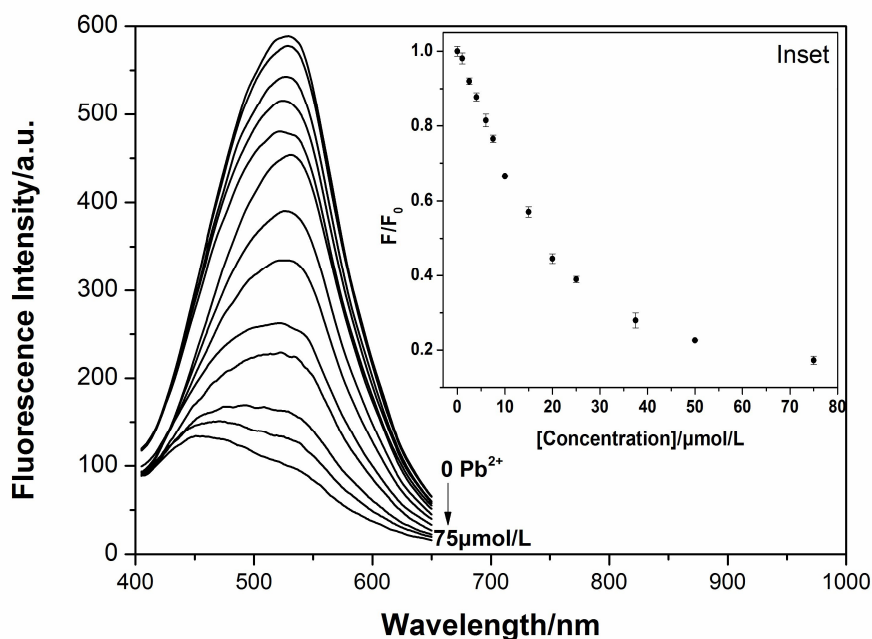
187 To generate a sensitive and stable nanosensor with a low detection limit for sulfide, it is  
 188 significant to choose the suitable material in the sensor fabrication process. So we investigated the  
 189 quenching ability to the BSA-CdS QDs by several commonly mental ions including Pb<sup>2+</sup>, Hg<sup>2+</sup>,

190  $\text{Cu}^{2+}$ ,  $\text{Ag}^+$ ,  $\text{Ca}^{2+}$ ,  $\text{Mn}^{2+}$ ,  $\text{Na}^+$ ,  $\text{Mg}^{2+}$ ,  $\text{Fe}^{3+}$ ,  $\text{Fe}^{2+}$ ,  $\text{Cd}^{2+}$  and  $\text{Zn}^{2+}$ . The FL intensity of BSA-CdS QDs  
191 after addition of 10  $\mu\text{mol/L}$   $\text{Pb}^{2+}$  or 50  $\mu\text{mol/L}$  other metal ions were shown in Fig. 2(B). The  
192 results demonstrated that  $\text{Pb}^{2+}$  could cause the biggest fluorescence quenching of the BSA-CdS  
193 QDs. Compared with  $\text{Pb}^{2+}$ ,  $\text{Hg}^{2+}$  and  $\text{Cu}^{2+}$  showed a relatively low FL quenching ability. Though  
194  $\text{Cu}^{2+}$  was always used for fabricating the sensor for sulfide, the  $\text{Cu}^{2+}$ -based sensor for  $\text{S}^{2-}$   
195 recognition would be seriously interfered with the cyanide.<sup>28,29</sup> Little change is observed when the  
196 BSA-CdS QDs was mixed with other metal ions ( $\text{Ag}^+$ ,  $\text{Ca}^{2+}$ ,  $\text{Mn}^{2+}$ ,  $\text{Na}^+$ ,  $\text{Mg}^{2+}$ ,  $\text{Fe}^{3+}$ ,  $\text{Fe}^{2+}$ ,  $\text{Cd}^{2+}$  and  
197  $\text{Zn}^{2+}$ ) even with a higher concentration (50 $\mu\text{mol/L}$ ) than  $\text{Pb}^{2+}$  (10 $\mu\text{mol/L}$ ), indicating the approach  
198 offers excellent selectivity towards  $\text{Pb}^{2+}$  ions. Therefore,  $\text{Pb}^{2+}$  was selected to fabricate the sulfide  
199 sensor.

200 In this work, the effect of the solution pH on the fluorescence intensity of the BSA-CdS QDs  
201 and  $\text{Pb}^{2+}$ /BSA-CdS QDs was investigated. The BSA, the stabilizer of CdS QDs in this study, had a  
202 pI equal to 4.8. Therefore, BSA-CdS QDs was electronegative when the pH value higher than 4.8,  
203 which could enhance the electrostatic interaction between BSA and  $\text{Pb}^{2+}$ . As shown in Figure 2(C),  
204 it could be seen that the FL intensity of BSA-CdS QDs increased with the increase of the pH value  
205 in the range from 6.2 to 8.2 and kept a relatively stable when the pH value was higher than 8.2.  
206 The FL intensity of  $\text{Pb}^{2+}$ /BSA-CdS QDs increased slowly when the pH value increased from 6.2 to  
207 9.0. The quenching ability of  $\text{Pb}^{2+}$  to BSA-CdS QDs reached the maximum value at pH 8.2.  
208 Therefore, pH value 8.2 was adopted in the further experiments.

209 The effect of incubation time on the fluorescence intensity of BSA-CdS QDs in the  
210 presence of 7.5  $\mu\text{mol/L}$   $\text{Pb}^{2+}$  was studied. The result in Fig. 2(D) showed that the quenching effect  
211 of  $\text{Pb}^{2+}$  on the fluorescence of BSA-CdS QDs was completed within 80 s and keep almost constant  
212 until 180 s. To ensure the completeness of fluorescence quenching of BSA-CdS QDs, we chose  
213 the 120s as the optimum incubation time.

### 214 **3.3 The quenching effect of $\text{Pb}^{2+}$ on the fluorescence of BSA-CdS QDs**



215

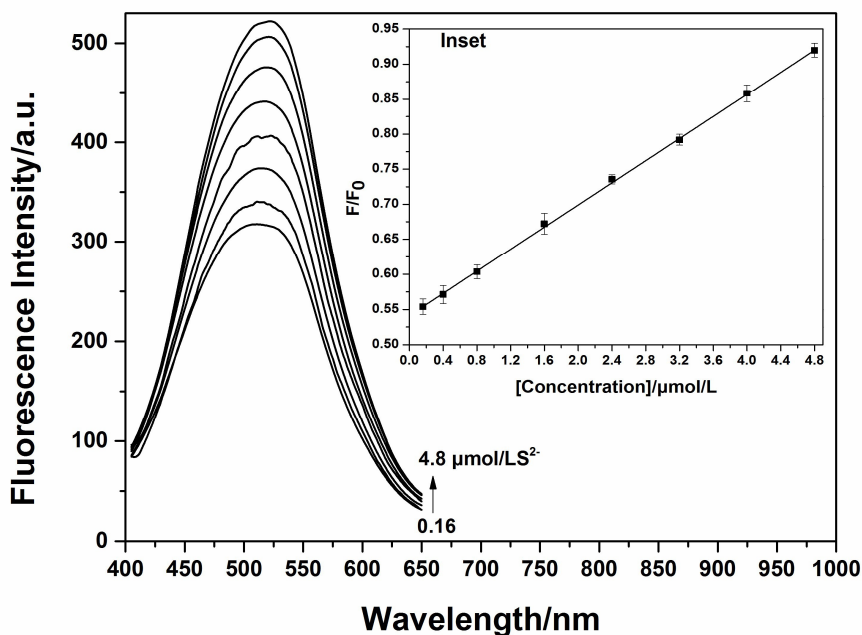
216 **Fig. 3** The fluorescence spectra of BSA-CdS QDs in the presence of different concentrations of  
217 Pb<sup>2+</sup>. The concentrations of Pb<sup>2+</sup> is 0, 1, 2.5, 4, 6, 7.5, 10, 15, 20, 25, 37.5, 50 and 75 μmol/L,  
218 respectively. The inset showed the relationship between F/F<sub>0</sub> and the concentration of Pb<sup>2+</sup>. F and  
219 F<sub>0</sub> were the fluorescence intensity of BSA-CdS QDs in the presence and absence of Pb<sup>2+</sup>,  
220 respectively.

221

222 In this work, we studied the quenching effect of Pb<sup>2+</sup> on the fluorescence of BSA-CdS QDs. As  
223 shown in Fig. 3, after the addition of Pb<sup>2+</sup> to the BSA-CdS QDs system, the FL intensity of  
224 BSA-CdS QDs at 529 nm was gradually decreased with the increasing concentration of Pb<sup>2+</sup>,  
225 which was due to a charge transfer process between Pb<sup>2+</sup> and BSA-CdS QDs. Also, a blue shift  
226 was observed when the Pb<sup>2+</sup> concentration was higher than 20 μmol/L, which was a consequence  
227 of the change of quantum confinement of the QDs.<sup>30,31</sup> The Inset in Fig. 3 showed that the relative  
228 fluorescence intensity F/F<sub>0</sub> (F and F<sub>0</sub> were the fluorescence intensity of BSA-CdS QDs in the  
229 presence and absence of Pb<sup>2+</sup>, respectively) and the concentration of Pb<sup>2+</sup> exhibited a linear  
230 relationship in the range of 1 - 20 μmol/L. We chose 15 μmol/L Pb<sup>2+</sup> to fabricate the nanosensor for  
231 sulfide anions detection.

232

## 233 3.4 Fluorescence detection of sulfide anions



234  
 235 **Fig. 4** The fluorescence spectra of BSA-CdS QDs/ $Pb^{2+}$  system in the presence of different  
 236 concentrations of  $S^{2-}$ . The concentrations of  $S^{2-}$  is 0.16, 0.4, 0.8, 1.6, 2.4, 3.2, 4.0 and 4.8  $\mu\text{mol/L}$ ,  
 237 respectively. The concentrations of  $Pb^{2+}$  was 15  $\mu\text{mol/L}$ . The inset showed the relationship  
 238 between  $F/F_0$  and the concentration of  $S^{2-}$  (from 0.16 to 4.8  $\mu\text{mol/L}$ ).  $F_0$  and  $F$  were the FL  
 239 intensity of BSA-CdS QDs and  $Pb^{2+}$ /BSA-CdS QDs system after the addition of  $S^{2-}$ , respectively.

240

241 It is well-known that  $Pb^{2+}$  can coordinate with sulfide anions to form the stable species. As the  
 242 stability constant of the PbS formed by  $S^{2-}$  and  $Pb^{2+}$  is larger than that of the complex of  $Pb^{2+}$  and  
 243 BSA-CdS QDs, thus the  $Pb^{2+}$ /BSA-CdS system could give some response to the target  $S^{2-}$  anions.  
 244  $S^{2-}$  anions can snatch the  $Pb^{2+}$  from the BSA-CdS QDs to form more stable PbS and restore the  
 245 fluorescence of BSA-CdS QDs to “turn on” state. Fig. 4 shows the evolution of fluorescence  
 246 spectra of  $Pb^{2+}$ /BSA-CdS QDs system with increasing  $S^{2-}$  concentration under the optimum  
 247 experimental conditions. It could be seen that the FL intensity of  $Pb^{2+}$ /BSA-CdS system obviously  
 248 restored when  $S^{2-}$  concentration increased from 0 to 6.4  $\mu\text{mol/L}$ . Furthermore, Inset in Fig. 4  
 249 showed that there was a good linear relationship between the relative fluorescence intensity ratio  
 250  $F/F_0$  and the  $S^{2-}$  concentration in the range from 0.16  $\mu\text{mol/L}$  to 4.8  $\mu\text{mol/L}$ . The regression

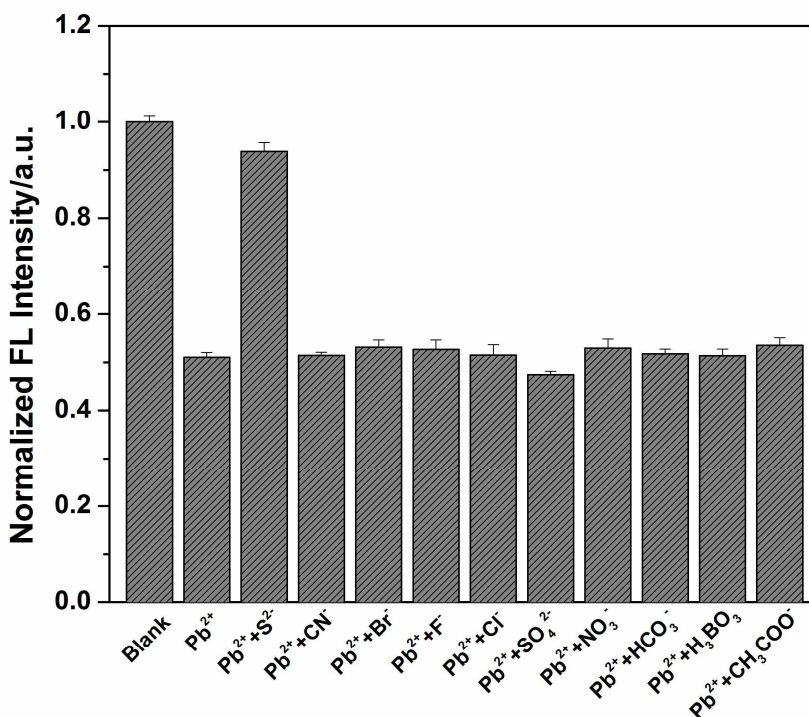
251 equation is

$$252 \quad F/F_0 = 0.54175 + 0.07906[S^{2-}], \mu\text{mol/L}$$

253 The corresponding regression coefficient ( $R^2$ ) is 0.999, and the detection limit for  $S^{2-}$  is 0.05  
 254  $\mu\text{mol/L}$ . Some analytical parameters in other methods for the detection of  $S^{2-}$  were listed in Table  
 255 S1.<sup>32-36</sup> Compared with those reports about  $S^{2-}$  assay, our present method offered a lower detection  
 256 limit. The result indicated that the proposed  $\text{Pb}^{2+}$ /BSA-CdS system was more sensitive for  $S^{2-}$   
 257 detection.

258

### 259 3.5 Interference study



260

261 **Fig. 5** Fluorescence restored behavior of 50 $\mu\text{L}$  BSA-CdS QDs in the presence of 15 $\mu\text{mol/L}$   $\text{Pb}^{2+}$   
 262 and 5  $\mu\text{mol/L}$   $\text{S}^{2-}$  or 100  $\mu\text{mol/L}$  potential coexisting anions. Bars: (1) BSA-CdS QDs only; (2)  
 263  $\text{Pb}^{2+}$ ; (3)  $\text{Pb}^{2+} + \text{S}^{2-}$ ; (4)  $\text{Pb}^{2+} + \text{CN}^-$ ; (5)  $\text{Pb}^{2+} + \text{Br}^-$ ; (6)  $\text{Pb}^{2+} + \text{F}^-$ ; (7)  $\text{Pb}^{2+} + \text{Cl}^-$ ; (8)  $\text{Pb}^{2+} + \text{SO}_4^{2-}$ ; (9)  
 264  $\text{Pb}^{2+} + \text{NO}_3^-$ ; (10)  $\text{Pb}^{2+} + \text{HCO}_3^-$ ; (11)  $\text{Pb}^{2+} + \text{H}_3\text{BO}_3$ ; (12)  $\text{Pb}^{2+} + \text{CH}_3\text{COO}^-$ . Reaction condition: 10  
 265 mmol/L Tris-HCl buffer solution (pH 8.2) at 25 $^\circ\text{C}$ .

266

267 Selectivity is a very important parameter to evaluate the performance of a new sensor, a highly

268 selective response to the target over other potentially competing species is necessary. Therefore,  
269 we further evaluated the selectivity of our nanosensor with various coexistence anions added. In  
270 order to investigate the influence of different coexisting anions on the fluorescence intensity of  
271  $\text{Pb}^{2+}$ /BSA-CdS, a series of 100  $\mu\text{mol/L}$  anions including  $\text{CN}^-$ ,  $\text{Br}^-$ ,  $\text{F}^-$ ,  $\text{Cl}^-$ ,  $\text{NO}_3^-$ ,  $\text{SO}_4^{2-}$ ,  $\text{HCO}_3^-$ ,  
272  $\text{H}_3\text{BO}_3$  and  $\text{CH}_3\text{COO}^-$  were introduced to  $\text{Pb}^{2+}$ /BSA-CdS system. As shown in Fig. 5, the  
273 fluorescence of BSA-CdS QDs was quenched after the addition of  $\text{Pb}^{2+}$ . Only  $\text{S}^{2-}$  had a highly  
274 specific response to  $\text{Pb}^{2+}$ /BSA-CdS complex and the fluorescence of CdS QDs could be  
275 effectively restored. The other anions had little ability to recover the FL intensity of BSA-CdS  
276 QDs quenched by  $\text{Pb}^{2+}$  even with a 20 times higher concentration than that of sulfide. The results  
277 showed that this sulfide detection system could provide well ability in resisting interference.

278

### 279 3.6 Analytical applications

280 To further investigate the practical applications of this method, the detection of sulfide in lake  
281 water was carried out. The classical methylene blue (MB) colorimetric method, a standard method  
282 for hydrogen sulfide determination in natural water, was used as a contrast method to detect sulfide  
283 in lake water samples.<sup>37, 38</sup> The average recovery test was made by using the standard addition  
284 method, and the results were listed in Table S2. From Table S2, it could be seen that the results  
285 obtained by the proposed fluorescence method are in good agreement with those obtained by the  
286 conventional method. The RSD was lower than 3.7%, and the average recoveries of sulfide in the  
287 real samples was in the range of 100–104%. All the obtained results indicated that this method has  
288 potential in environmental applications for sulfide detection.

289

## 290 4. Conclusion

291 In summary, a novel nanosensor,  $\text{Pb}^{2+}$ /BSA-CdS complex, had been designed for the recognition  
292 and detection of sulfide. The fluorescent BSA-CdS QDs could be quenched by  $\text{Pb}^{2+}$  due to the  
293 charge transfer between BSA-CdS QDs and  $\text{Pb}^{2+}$ . Subsequent addition of  $\text{S}^{2-}$  to  $\text{Pb}^{2+}$ /BSA-CdS

294 solution lead to the fluorescence recovery of BSA-CdS QDs through forming the stable PbS  
295 compound. It constituted a “turn off-on” type fluorescence sensing system. Compared with the  
296 literatures about S<sup>2-</sup> assay, our present method offered a fast and convenient analytical method by  
297 using CdS QDs. This method provides an alternative for the sensitive and selective detection of  
298 sulfide.

### 299 **Acknowledgements**

300 This work was financially supported by the National Natural Science Foundation of China (No.  
301 21075050, No. 21275063) and the science and technology development project of Jilin province,  
302 China (No. 20110334).

303

### 304 **References**

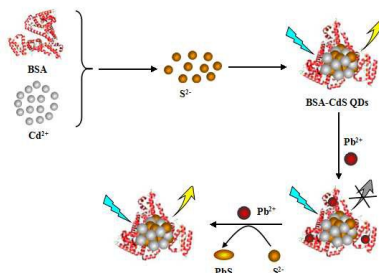
- 305 1 X. F. Yang, L. Wang, H. Xu, M. Zhao, *Analytica Chimica Acta*, 2009, 1, 91-95.
- 306 2 C. Kar, G. Das, *Journal of Photochemistry and Photobiology a-Chemistry*, 2013, 251,  
307 128-133.
- 308 3 X. Lou, H. Mu, R. Gong, E. Fu, J. Qin, Z. Li, *Analyst*, 2011, 4, 684-687.
- 309 4 L. Tang, X. Dai, M. Cai, J. Zhao, P. Zhou, Z. Huang, *Spectrochimica Acta Part a-Molecular  
310 and Biomolecular Spectroscopy*, 2014, 122, 656-660.
- 311 5 B. Sen, M. Mukherjee, S. Pal, K. Dhara, S. K. Mandal, A. R. Khuda-Bukhsh, P.  
312 Chattopadhyay, *Rsc Advances*, 2014, 29, 14919-14927.
- 313 6 H. Huang, Q. Li, J. Wang, Z. Li, X. F. Yu, P.K. Chu, *Plasmonics*, 2014, 1, 11-16.
- 314 7 F. Zheng, M. Wen, F. Zeng, S. Wu, *Sensors and Actuators B-Chemical*, 2013, 188,  
315 1012-1018.
- 316 8 R. Zhang, X. Yu, Y. Yin, Z. Ye, G. Wang, J. Yuan, *Analytica Chimica Acta*, 2011, 691, 83-88.
- 317 9 Z. Ye, X. An, B. Song, W. Zhang, Z. Dai, J. Yuan, *Dalton Transactions*, 2014, 34,  
318 13055-13060.
- 319 10 M. Li, Q. Liang, M. Zheng, C. Fang, S. Peng, M. Zhao, *Dalton Transactions*, 2013, 37,  
320 13509-13515.
- 321 11 K. Wang, H. Peng, N. Ni, C. Dai, B. Wang, *Journal of Fluorescence*, 2014, 1, 1-5.
- 322 12 N. Adarsh, M. S. Krishnan, D. Ramaiah, *Analytical chemistry*, 2014, 18, 9335-9342.

- 323 13 B. Chen, P. Wang, Q. Jin, X. Tang, *Organic & Biomolecular Chemistry*, 2014, 30,  
324 5629-5633.
- 325 14 Z. Wu, Y. Feng, B. Geng, J. Liu, X. Tang, *RSC Advances*, 2014, 57, 30398-30401.
- 326 15 J. Bae, J. Choi, T. J. Park, S. K. Chang, *Tetrahedron Letters*, 2014, 6, 1171-1174.
- 327 16 Q. Huang, X. F. Yang, H. Li, *Dyes and Pigments*, 2013, 3, 871-877.
- 328 17 M. A. Ali, S. Srivastava, M. K. Pandey, V. V. Agrawal, R. John, B. D. Malhotra, *Analytical  
329 chemistry*, 2014, 3, 1710-1718.
- 330 18 L. Saa, J. M. Mato, V. Pavlov, *Anal Chem*, 2012, 21, 8961-8965.
- 331 19 M. Vazquez-Gonzalez, C. Carrillo-Carrion, *Journal of biomedical optics*, 2014, 10,  
332 101503-101503.
- 333 20 A. H. Gore, S. B. Vatre, P. V. Anbhule, S. H. Han, S. R. Patil, G. B. Kolekar, *Analyst*, 2013, 5,  
334 1329-1333.
- 335 21 H. R. Rajabi, M. Shamsipur, A. A. Khosravi, O. Khani, M. H. Yousefi, *Spectrochimica Acta  
336 Part a-Molecular and Biomolecular Spectroscopy*, 2013, 107, 256-262.
- 337 22 H. Matsumoto, T. Sakata, H. Mori, H. Yoneyama, *The Journal of Physical Chemistry*, 1996,  
338 32, 13781-13785.
- 339 23 G. Garai-Ibabe, L. Saa, V. Pavlov, *Analytical chemistry*, 2013, 11, 5542-5546.
- 340 24 W. Tedsana, T. Tuntulani, W. Ngeontae, *Analytica Chimica Acta*, 2013, 783, 65-73.
- 341 25 S. S. Liji Sobhana, M. Vimala Devi, T. P. Sastry, A. Mandal, *J Nanopart Res*, 2011, 13  
342 1747-1757.
- 343 26 S. Liu, F. Shi, L. Chen, X. Su, *Talanta*, 2013, 116, 870-875.
- 344 27 Y. Huang, Y. Luo, W. Zheng, T. Chen, *Acs Applied Materials & Interfaces*, 2014, 21,  
345 19217-19218.
- 346 28 Y. Wang, H. Sun, L. Hou, Z. Shang, Z. Dong, W. Jin, *Analytical Methods*. 2013, 20,  
347 5493-5500.
- 348 29 X. Lou, H. Mu, R. Gong, E. Fu, J. Qin, Z. Li, *Analyst*, 2011, 4, 684-687.
- 349 30 B. B. Campos, M. Algarra, B. Alonso, C. M. Casado, J. C. G. Esteves da Silva, *Analyst*, 2009,  
350 12, 2447-2452.
- 351 31 L. Zhang, X. Lou, Y. Yu, J. Qin, Z. Li, *Macromolecules*, 2011, 13, 5186-5193.
- 352 32 W. Zhong, C. Zhang, Q. Gao, H. Li, *Microchimica Acta*, 2011, 176, 101-107.



- 353 33 J. Zhang, X. Xu, Y. Yuan, C. Yang, X. Yang, *Acs Applied Materials & Interfaces*, 2011, 8,  
354 2928-2931.
- 355 34 B. H. Zhang, F. Y. Wu, Y. M. Wu, X. S. Zhan, *Journal of Fluorescence*, 2010, 1, 243-250.
- 356 35 L. E. Santos-Figueroa, C. de la Torre, S. El Sayed, F. Sancenon, R. Martinez-Manez, A. M.  
357 Costero, S. Gil, M. Parra, *European Journal of Inorganic Chemistry*, 2014, 1, 41-45.
- 358 36 J. Liu, J. Chen, Z. Fang, L. Zeng, *Analyst*, 2012, 23, 5502-5505.
- 359 37 S. B. Xue, *Science and Technology Innovation Herald*, 2010, 31, 80-80.
- 360 38 J. F. da Silveira Petrucci, A. A. Cardoso, *Microchemical Journal*, 2013, 106, 368-372.
- 361

## Table of Contents



Schematic illustration of the BSA-CdS QDs-based sensing system for sulfide detection